ORIGINAL ARTICLE





Secreted lumican from the tumor microenvironment potentiates HCC stemness and progression

Kristy Kwan-Shuen Chan¹ | Cheuk-Yan Wong¹ | Kwan-Yung Au¹ | Long-Hin Suen¹ | Wai-Wai Yip¹ | Jing-Mian Zhang¹ | Eva Yi-Man Fung² | Terence Kin-Wah Lee^{3,4} | Irene Oi-Lin Ng^{1,5} | Tan-To Cheung^{5,6} | Regina Cheuk-Lam Lo^{1,5} ©

Correspondence

Regina Cheuk-Lam Lo, Department of Pathology, The University of Hong Kong, Queen Mary Hospital, Pokfulam, Hong Kong, China.

Email: loregina@hku.hk

Abstract

Background: Extracellular matrix proteins are tightly linked to cancer progression. HCC frequently arises from chronic liver diseases with varying degrees of parenchymal fibrosis. Herein, we aimed to investigate the roles of secreted lumican, an extracellular matrix proteoglycan, in HCC.

Methods: Lumican expression in clinical liver tissue samples was analyzed. In vitro and in vivo functional assays were performed with cell lines. Co-culture systems were adopted to examine the roles of lumican in the interaction between HCC cells and liver fibroblasts. Downstream mechanisms were interrogated by transcriptomic and proteomic profiling.

Results: Analyses of single-cell RNA-sequencing datasets collectively revealed high lumican expression in liver fibroblasts. Lumican expression was elevated in liver tissues with advanced fibrosis, and a higher lumican level in the non-tumor liver tissue was a poor prognosticator of HCC. Functionally, recombinant human lumican (rhLUM) promoted migration, invasion, and self-renewal of HCC cells, and enhanced angiogenesis in vitro. These effects were abrogated by anti-lumican antibody. The paracrine actions of lumican in the interplay between HCC cells and liver fibroblasts were supported with co-culture models, in which lumican was manipulated by genetic or antibody approaches. In vivo, recombinant lumican promoted

Abbreviations: anti-LUM, anti-lumican antibody; bFGF, basic fibroblast growth factor; CCl₄, carbon tetrachloride; CCMR, Centre for Comparative Medicine Research; CM, conditioned medium; CPTAC-LIHC, Clinical Proteomic Tumor Analysis Consortium Liver Hepatocellular Carcinoma; Ctrl, control; CULATR, Committee on the Use of Live Animals in Teaching and Research; DEG, differentially expressed gene; DEP, differentially expressed protein; ECM, extracellular matrix; FC, fold change; FDR, false discovery rate; FFPE, formalin-fixed paraffin-embedded; GPC3, glypican-3; GO, Gene Ontology; LF, liver fibroblasts; LF-CM, conditioned medium of liver fibroblasts; LUM, lumican; PDX, patient-derived xenograft; rhLUM, recombinant human lumican; rmLUM, recombinant mouse lumican; RNA-seq, RNA-sequencing; siCtrl, negative control siRNA; siLUM, lumican siRNA; sLUM, secreted lumican; TCGA-LIHC, The Cancer Genome Atlas Liver Hepatocellular Carcinoma; T-IC, tumor-initiating cell.

Kristy Kwan-Shuen Chan and Cheuk-Yan Wong contributed equally to this work.

Supplemental Digital Content is available for this article. Direct URL citations are provided in the HTML and PDF versions of this article on the journal's website, www.hepcommiournal.com.

This is an open access article distributed under the terms of the Creative Commons Attribution-Non Commercial-No Derivatives License 4.0 (CCBY-NC-ND), where it is permissible to download and share the work provided it is properly cited. The work cannot be changed in any way or used commercially without permission from the journal.

Copyright © 2025 The Author(s). Published by Wolters Kluwer Health, Inc. on behalf of the American Association for the Study of Liver Diseases.

¹Department of Pathology, School of Clinical Medicine, LKS Faculty of Medicine, The University of Hong Kong, Hong Kong, China

²Department of Chemistry, Faculty of Science, The University of Hong Kong, Hong Kong, China

³Department of Applied Biology and Chemical Technology, The Hong Kong Polytechnic University, Hong Kong, China

⁴State Key Laboratory of Chemical Biology and Drug Discovery, The Hong Kong Polytechnic University, Hong Kong, China

⁵State Key Laboratory of Liver Research, The University of Hong Kong, Hong Kong, China

⁶Department of Surgery, School of Clinical Medicine, LKS Faculty of Medicine, The University of Hong Kong, Hong Kong, China

neovascularization and tumor incidence. Profiling results revealed the enrichment of Wnt signaling, and mechanistic dissection uncovered the crosstalk between PI3K/AKT and Wnt/ β -catenin pathways in rhLUM-treated HCC cells.

Conclusions: Secreted lumican promotes HCC self-renewal, tumor initiation, and progression by activating the AKT/GSK3 β / β -catenin signaling cascade. Targeting secreted lumican is a potential therapeutic strategy for HCC.

Keywords: extracellular matrix proteins, fibroblasts, liver cancer

INTRODUCTION

HCC is the major type of primary liver cancer and a topranking cancer worldwide. The high propensity for intrahepatic recurrence and extrahepatic metastasis is a treatment hurdle even after surgical resection of the tumor. Encouraging results from the latest developments in targeted therapies substantiate further exploration of molecular targets that potentially expand the treatment modalities for this aggressive cancer.

Recent advances in medical research have uncovered the role of non-tumor cells among the tumor milieu in fostering tumorigenesis and cancer progression. This concept possibly carries special implications in HCC, since the majority of HCC arise in a background of chronic liver diseases, in which persistent inflammation and progressive fibrosis of the parenchyma are characteristic. Moreover, the chronic fibroinflammatory milieu exists before, during, and after HCC development and constitutes a unique and special microenvironment of this cancer. Notably, the degree of liver fibrosis in the non-tumor liver tissue per se is a prognostic factor for HCC described in the American Joint Committee on Cancer staging system. In line with this, studies evaluating liver fibrosis by histological assessment, [1] surrogate biomarker for liver fibrosis, FIB-4,[2] and liver stiffness measurement[3] collectively indicated that a high degree of fibrosis in the background liver tissue is a poor prognosticator for HCC. While this could be attributed to poor liver reserve, whether direct protumorigenic mechanisms are in play remains to be interrogated. The crosstalk between constituent cells in fibrosis and HCC cells could be important in the comprehensive understanding of molecular events implicated in liver cancer. This prompted us to revisit the extracellular matrix (ECM) components in liver fibrosis, specifically whether any of these components could be exhibiting pro-tumorigenic effects.

Proteoglycans are pivotal elements of the ECM. Interestingly, apart from serving as the constituent components of the fibrogenic process, these proteins

functional role in promoting progression.^[4] A representative example is glypican-3 (GPC3), a transmembrane proteoglycan. GPC3 is overexpressed in the tumor and serum samples of HCC patients. Lumican, a member of the extracellular proteoglycans, is located on human chromosome 12g21.33, comprising 338 amino acids with a molecular weight of ~40 kDa. Of note, lumican was found to play a pivotal role in fibrosis by regulating matrix assembly and enhancing collagen fibril stability. In the liver, lumicannull mice showed a marked reduction in liver fibrosis, portraying lumican as a prerequisite for liver fibrosis. [5] In human clinical samples, upregulation of lumican at the mRNA level was initially reported in chronic hepatitis B liver tissue. [6] Lumican overexpression at the protein level was then identified in the liver tissues from individuals with non-alcoholic fatty liver disease.[7] In a later study, the potential role of lumican as a serum surrogate biomarker for liver fibrosis associated with non-alcoholic fatty liver disease was proposed.[8]

Functional studies on intracellular lumican revealed both pro-tumorigenic and anti-tumorigenic roles in human cancers. [9-11] Manipulation of intracellular lumican in cancer cells resulted in various phenotypic alterations depending on tumor origin. [12-18] In contrast, fewer studies focused on the secreted form of lumican, of which the role in human cancers also appears divergent in a tissue-specific manner. It was reported that secreted lumican (sLUM) suppresses the growth of pancreatic cancer, and that a high extracellular lumican expression in the tumor tissue is associated with better survival outcome.[19] In gastric cancer, a higher expression in the tumor stroma was associated with aggressive clinicopathological features, and functionally sLUM demonstrates a pro-tumorigenic effect in vitro and in vivo.[20] To date, while being an integral ECM protein, the functional significance of sLUM in HCC remains poorly understood.

In this study, we investigated the functional roles of sLUM in HCC. From our expression analyses of clinical samples, lumican was remarkably expressed in liver fibroblasts. Lumican expression was elevated in liver tissues with advanced fibrosis, and a higher lumican level in the non-tumor liver tissue was a poor prognosticator of HCC. Functionally, we demonstrated that sLUM promoted self-renewal, tumor initiation, and metastatic potential in HCC and enhanced angiogenesis. Mechanistically, sLUM triggered the AKT/GSK3 β / β -catenin signaling cascade and induced nuclear localization of β -catenin.

METHODS

Clinical samples

The study was conducted in accordance with both the Declarations of Helsinki. Use of clinical samples was approved by the Institutional Review Board of The University of Hong Kong/Hospital Authority Hong Kong West Cluster (HKU/HA HKW IRB: UW11-424) with waiver of written informed consent. Clinical HCC tissue samples were obtained from liver resection specimens at Queen Mary Hospital, Hong Kong, and were either snap-frozen in liquid nitrogen and stored at −80 °C or processed into formalin-fixed paraffin-embedded blocks.

Carbon tetrachloride-induced liver fibrosis mouse model

Animal experiments were adhered to the ARRIVE Guidelines, conducted following review and approval from the Committee on the Use of Live Animals in Teaching and Research (CULATR) of HKU and under licence from the Hong Kong SAR Government's Department of Health (CULATR approval numbers: 4504-17, 5498-20, 5844-21, 23-215). Five- to 7-weekold male C57BL/6J mice (RRID: IMSR JAX:000664) originally sourced from The Jackson Laboratory were bred under an AAALAC International-accredited program at the Centre for Comparative Medicine Research (CCMR) under specific pathogen-free conditions. All mice were housed in a specific pathogen-free and temperature-controlled environment providing a 12:12hour light:dark cycle and were fed ad libitum with LabDiet 5LG4 (breeding diet) and LabDiet 5053 (maintenance diet) manufactured by the Jackson Laboratory. All mice were randomly divided into 2 groups (corn oil or CCl₄ group; 5 mice/group). To induce liver fibrosis, mice were injected intraperitoneally with carbon tetrachloride (CCI₄) (0.2 ml/kg of body weight; MilliporeSigma) diluted in corn oil (MilliporeSigma) twice per week. Liver tissue of each mouse was harvested and snap-frozen in liquid nitrogen or fixed in 10% neutral buffered formalin. Formalin-fixed paraffinembedded mouse liver tissue was sectioned and stained with hematoxylin and eosin and trichrome stain. The severity of liver fibrosis was determined by a pathologist. Images were captured with Nanozoomer S210 (Hamamatsu Photonics, RRID: SCR_023760).

Subcutaneous injection xenograft model

Male NOD.CB17-Prkdcscid/J (NOD/SCID) mice at 6-8 weeks old, originally sourced from The Jackson Laboratory, were bred under an AAALAC International-accredited program at the CCMR, HKU under specific pathogen-free conditions. Animals were housed in individually ventilated cages under a 12:12 dark-light cycle within environmentally controlled rooms and were fed ad libitum with LabDiet 5LG4 (breeding diet) and LabDiet 5053 (maintenance diet) manufactured by the Jackson Laboratory. Patient-derived xenograft (PDX1) was established with an HCC resection specimen collected from Queen Mary Hospital, Hong Kong, as previously described. [21,22] For propagation, PDX1 tumor was harvested from tumor-bearing mice and was processed to a single-cell suspension in the presence of Liberase (10 µg/mL, Roche Diagnostics), DNase I (250 µg/mL, Roche Diagnostics), and Y27632 (15 µM, MedChemExpress) using a gentleMACS dissociator (Miltenyi Biotec). Single-cell suspension was collected through a 100 µm nylon cell strainer (SPL Life Sciences). Cell viability and cell counting were assessed using the trypan blue exclusion method. HCC cells (1000 cells for MHCC97L, 5000 cells for Huh7, and 10,000 cells for HCC PDX1 in 100 µL serum-free medium and Matrigel, 1:1) were subcutaneously injected into the dorsal flank of the mice. Mice were randomized into 2 groups [Ctrl and recombinant human lumican (rhLUM)]. One (for MHCC97L and PDX1) or 2 (for Huh7) weeks post-cell injection, PBS, or rhLUM (100 µg/kg) was subcutaneously injected to the tumor injection site of the Ctrl or rhLUM group twice per week for a total of 8 (for PDX1), 13 (for Huh7) or 15 (for MHCC97L) injections. Tumor incidence was monitored, and tumors were harvested on day 35 post-cell injection for PDX1, day 84 post-cell injection for Huh7 cells, and day 74 post-cell injection for MHCC97L cells. Tumorinitiating cell (T-IC) frequency was calculated using extreme-limiting-dilution analysis.[23]

In vivo Matrigel plug assay

Five-week to 7-week-old male BALB/cAnN-nu (nude) mice originally sourced from The Charles River Lab (BioLASCO) were bred under an AAALAC International-accredited program at the CCMR under specific pathogen-free conditions. All mice were housed in a specific pathogen-free and temperature-controlled environment providing 12:12-hour light:dark cycle and were

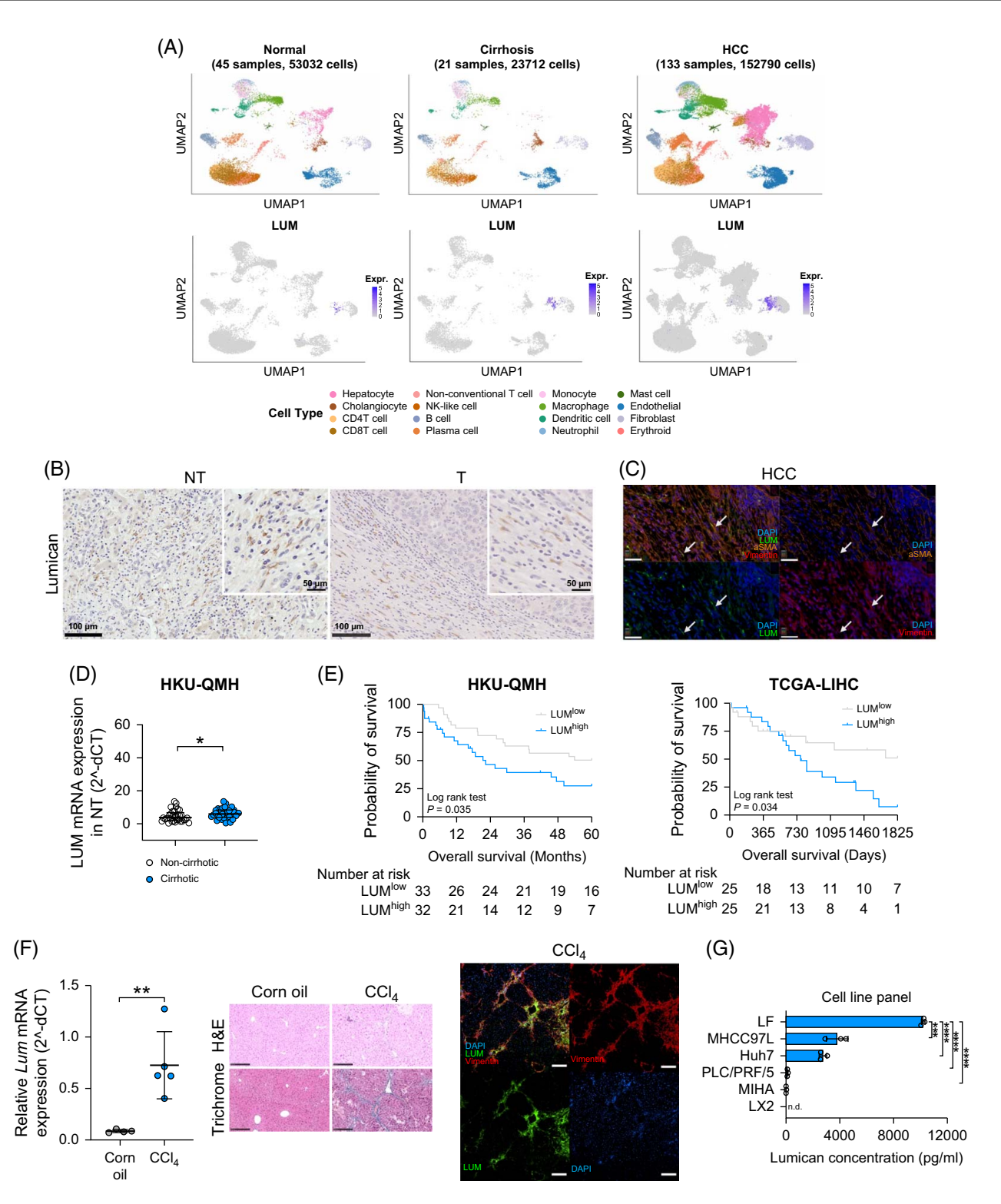


FIGURE 1 Lumican is highly expressed in liver fibroblasts. (A) UMAP plots of the cell clusters and lumican expression analyzed from integrated normal liver, cirrhotic liver, and HCC tissue datasets using the GepLiver database (http://www.gepliver.org/#/explore). Graph layouts were modified based on the originals, with the cell type annotation underneath the lumican expression UMAP plots. (B) Immunohistochemical staining for lumican in tumor (T) tissue and non-tumor (NT) liver tissue from HCC clinical samples. Scale bar of full-size image: 100 μm. Scale bar of inset: 50 μm. (C) Multiplex fluorescence immunohistochemistry of lumican (LUM), α-smooth muscle actin (αSMA), and vimentin in a clinical HCC sample. LUM (green), αSMA (orange), vimentin (red), and DAPI (blue). Representative cells with colocalization of LUM, αSMA, and vimentin were indicated by the white arrows. Scale bar: 50 μm. (D) Lumican mRNA expression in non-tumor (NT) liver tissue from 65 HCC clinical samples. Samples were categorized based on the status, non-cirrhotic (n = 33) versus cirrhotic (n = 32), of non-tumor liver tissue. Mann–Whitney *U* test. The line represents the median with the IQR. (E) Kaplan–Meier analysis of 5-year overall survival in HCC patients (HKU-QMH) stratified by median of lumican (LUM) mRNA expression level in non-tumor liver tissue. LUMlow (n = 33) and LUMhigh (n = 32) (left). Survival data are available in 65 HCC

patients. Kaplan–Meier analysis of 5-year overall survival in HCC patients (TCGA-LIHC) stratified by a median of lumican mRNA expression level in non-tumor liver tissue. LUMlow (n = 25) and LUMhigh (n = 25) (*right*). Log-rank test. (F) Lumican mRNA expression in liver tissue collected from corn oil-treated C57BL/6J mice (n = 4) and CCl₄-treated C57BL/6J mice (n = 5) (*left*). Representative image of H&E and trichrome stain of mouse liver tissue (*middle*). Scale bar: 250 μ m. Immunofluorescent staining for lumican and vimentin in fibrotic liver tissue from the mice (*right*). Scale bar: 500 μ m. Unpaired *t* test. The line represents mean \pm SD. (G) Lumican concentration (pg/mL) in conditioned medium collected from immortalized hepatocyte cell line (MIHA), liver fibroblasts (LF), HSC cell line (LX2), and HCC cell lines (n = 3). Unpaired *t* test. The line represents mean \pm SD. *p < 0.05, **p < 0.01, ***p < 0.001, and ****p < 0.0001; n.d., not detectable. Abbreviations: CCl₄, carbon tetrachloride; HKU-QMH, The University of Hong Kong—Queen Mary Hospital; LUM, lumican; NT, non-tumor; T, tumor; TCGA-LIHC, The Cancer Genome Atlas Liver Hepatocellular Carcinoma; UMAP, Uniform Manifold Approximation and Projection.

fed ad libitum with LabDiet 5LG4 (breeding diet) and LabDiet 5053 (maintenance diet) manufactured by the Jackson Laboratory. All mice were randomly divided into 2 or 3 groups [Ctrl, recombinant mouse lumican (rmLUM), or rmLUM+anti-lumican antibody (anti-LUM)]. A total of 300 µL growth factor reduced Matrigel (Corning Inc.) mixed with basic fibroblast growth factor (bFGF; MilloporeSigma; 250 ng/mL) supplemented with or without rmLUM (R&D Systems; 2 µg) or bFGF mixed with rmLUM and anti-LUM (2 µg; AF2745, R&D Systems; RRID: AB_2139496) followed by subcutaneous injection to the flank of nude mice. bFGF (250 ng/mL) mixed with or without rmLUM (2 µg) or bFGF mixed with rmLUM (2 μg) and anti-LUM (2 μg) was subcutaneously injected into the Matrigel plug of the Ctrl, rmLUM, or rmLUM+anti-LUM group, respectively, every other day. After 9 days, Matrigel plugs were removed, imaged, and fixed in 10% buffered formalin. Microvessel density was assessed by a pathologist. Images were captured with Nanozoomer S210 (Hamamatsu Photonics; RRID: SCR 023760).

Statistical analysis

The Shapiro–Wilk test was performed to assess the normality of the data. Continuous variables between 2 groups were compared using the Mann–Whitney U test for non-parametric data, and the unpaired t test for parametric data. Survival analyses were performed using the Kaplan–Meier method and were compared with the log-rank test. A 2-tailed p value of < 0.05 was considered statistically significant. Statistical analyses were performed using GraphPad Prism v8.2.1 (GraphPad Software Inc.; RRID: SCR_002798) or SPSS Statistics v25 (SPSS Inc.; RRID: SCR_016479).

Experimental details of cell culture, The Cancer Genome Atlas (TCGA) analysis and GepLiver single-cell RNA-sequencing analysis, multiplex fluorescence immunohistochemistry, immunofluorescent staining, establishment of transient lumican knockdown cells, preparation of conditioned medium, ELISA, immunohistochemical staining, reverse transcription-quantitative polymerase chain reaction, western blotting, co-immunoprecipitation, co-culture system, transwell migration and invasion assays, transendothelial migration assay, tube formation assay, tumorsphere formation assay, MTT assay, RNA

sequencing, bioinformatics and computational analyses, liquid chromatography–tandem mass spectrometry, Gene Ontology (GO) and Reactome gene set enrichment analysis are available in Supplemental Materials and Methods and Supplemental Table S3, http://links.lww.com/HC9/C59.

RESULTS

Lumican is highly expressed in liver fibroblasts

We first analyzed lumican expression from single-cell RNA-sequencing (RNA-seq) data using web-accessible database GepLiver, which integrated expression profiles of liver cells from 17 single-cell RNA-seq datasets deposited in Gene Expression Omnibus and Sequencing Read Archive databases. Lumican mRNA was remarkably expressed in fibroblasts residing in normal liver, cirrhotic liver, and HCC tissues (Figure 1A). Of note, lumican ranked as one of the top 10 most expressed marker genes in the extracellular matrix fibroblast cluster from the GepLiver database. To this end, immunohistochemical staining was performed in whole sections of our clinical liver tissue samples to verify the cell types expressing lumican. In non-tumor cirrhotic liver tissue, lumican expression was localized among the fibroblasts, while the hepatocytes showed negative staining. In HCC tumor tissue, lumican expression was observed in fibroblasts at the tumor edge as well as in some HCC cells by immunohistochemistry (Figure 1B). Moreover, multiplex fluorescence immunohistochemistry in clinical samples showed the colocalization of lumican with fibroblast markers α -smooth muscle actin and (Figure 1C). We further looked at the expression of lumican in paired tumor and non-tumor tissues from our in-house HCC clinical cohort, in which the vast majority of cases (61 of 65) were associated with chronic liver diseases. First, we observed that in the non-tumor liver tissue, lumican expression was significantly higher in the cirrhotic subset versus the non-cirrhotic subset (Figure 1D). Second, survival analyses were carried out to explore the clinical significance of lumican expression. Interestingly, a higher lumican level in the nontumor liver tissue was associated with worse 5-year

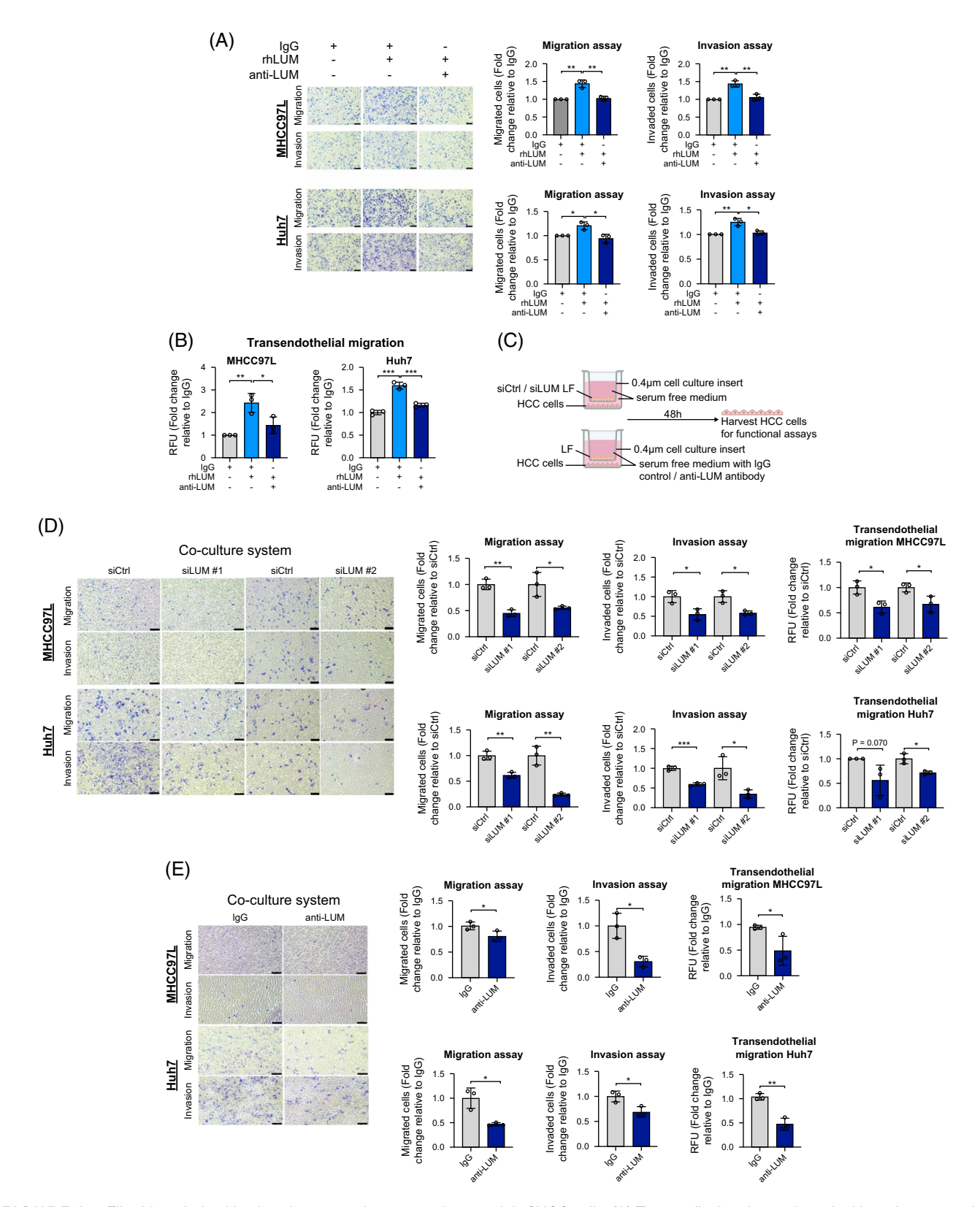


FIGURE 2 Fibroblast-derived lumican increases the metastatic potential of HCC cells. (A) Transwell migration and matrigel invasion assays in MHCC97L (upper) and Huh7 (lower) cells upon rhLUM (2 μ g/mL) or in combination of rhLUM (2 μ g/mL) and anti-LUM antibody (2 μ g/mL) treatment (n = 3). Unpaired t test. Data represents mean \pm SD. Scale bar: 200 μ m. (B) Transendothelial migration of MHCC97L (n = 3) and Huh7 cells treated with rhLUM (2 μ g/mL) or in combination of rhLUM and anti-LUM antibody (2 μ g/mL). Representative data of Huh7 is shown. The experiment was performed twice, each in triplicate. Unpaired t test. Data represents mean \pm SD. (C) Schematic diagram of the co-culture system. The figure is created with BioRender.com. (D) Transwell migration, Matrigel invasion assays, and transendothelial migration assays in MHCC97L (upper), Huh7 (lower) cells, or HCC cells co-cultured with siCtrl or siLUM liver fibroblasts (LFs). Representative data is shown for transwell assays. Scale

bar: 200 μ m. The experiment was performed at least twice, each in triplicate. Unpaired t test. Data represents mean \pm SD. (E) Transwell migration, Matrigel invasion assays, and transendothelial migration assay in MHCC97L (upper), Huh7 (lower) cells, or HCC cells co-cultured with LF treated with IgG control or anti-LUM antibody ($2 \mu g/mL$). Representative data is shown. Scale bar: 200 μ m. The experiment was performed twice, each in triplicate. Unpaired t test. Data represents mean \pm SD. Scale bar: 200 μ m. *p < 0.05, **p < 0.01, and ***p < 0.001. Abbreviations: anti-LUM, anti-lumican antibody; rhLUM, recombinant human lumican.

overall survival of HCC patients (Figure 1E), while lumican level in the matched tumor tissues did not show a statistically significant correlation (p = 0.592). The prognostic significance of lumican in the non-tumor liver tissue was supported by analysis of The Cancer Genome Atlas Liver Hepatocellular Carcinoma (TCGA-LIHC) cohort of HCC samples (Figure 1E). To corroborate the above observations, lumican mRNA expression was evaluated in the livers harvested from our CCl₄-induced liver fibrosis mouse model, in which C57BL/6J mice were treated with CCI₄ to induce liver fibrosis. Consistently, lumican was significantly elevated in the fibrotic liver tissue from the CCl₄-treated group, and colocalization of lumican and vimentin expressions was observed in the fibrotic regions (Figure 1F). In addition, sLUM was quantified in the conditioned medium (CM) of human liver cell lines, including liver fibroblasts (LFs), immortalized hepatocytes MIHA, HSC line LX2, and HCC cell lines (Huh7, PLC/PRF/5, and MHCC97L) by ELISA. In congruence, LF demonstrated a higher sLUM level versus other cell lines (Figure 1G).

Fibroblast-derived secreted lumican increases the metastatic potential of HCC

To gather insights on the effects of sLUM on HCC cells, rhLUM and anti-lumican antibody (anti-LUM) were employed. Before this, the toxicity of rhLUM and anti-LUM was assessed on liver cell lines. No significant cytotoxic effect was observed upon administration of rhLUM or anti-LUM (Supplemental Figures S1A, B, http:// links.lww.com/HC9/C59). Functionally, treatment of rhLUM to HCC cells augmented cell migration and invasion as tested by cell motility assay and Matrigel invasion assay, respectively. Besides, administration of anti-LUM abrogated the effects of migration and invasion conferred by rhLUM on HCC cells (Figure 2A). Following that, we carried out a transendothelial migration assay, which examines the ability of cancer cells to migrate across the endothelial layer, mimicking the intravasation step in metastasis. Transendothelial migration was enhanced upon rhLUM administration, and co-treatment with anti-LUM dampened this effect (Figure 2B). In an attempt to study the interaction between HCC cells and LF, which secreted an abundant amount of lumican, we proceeded to examine the effects of the conditioned medium of liver fibroblasts (LF-CM) on HCC cell properties. From our experiments, migration and invasion of HCC cells were enhanced by LF-CM compared with the untreated control. These effects were abrogated

by co-treatment with anti-LUM (Supplemental Figure S2, http://links.lww.com/HC9/C59). The interplay between LF and HCC cells was further evaluated with a co-culture system. HCC cells were co-cultured with LF transiently transfected with negative control siRNA (siCtrl) or 2 sequences of lumican siRNA (siLUM), followed by in vitro assays (Figure 2C). The reduction of sLUM concentration in CM collected from LF transfected with siLUM was confirmed (Supplemental Figure S3, http://links.lww.com/ HC9/C59). We observed suppressed migration, invasion, and transendothelial migration of HCC cells cocultured with lumican-silenced LF (Figure 2D). These findings were further consolidated by a second co-culture setup, in which HCC cells were co-cultured with LF supplemented with anti-LUM or IgG control before in vitro assays. In line with the previous results, cell migration, invasion, and transendothelial migration in HCC cells were dampened in the anti-LUM treatment group (Figure 2E).

Secreted lumican enhances angiogenesis

Next, we proceeded to study whether sLUM exerts any functional effects on neovascularization, another key process in cancer progression. To this end, an in vitro tube formation assay with HUVEC was carried out. The results demonstrated that rhLUM enhanced new vessel formation, and anti-LUM abrogated this angiogenic effect (Figure 3A). Similarly, using co-culture setups, reduced tube formation ability in the HUVEC was observed in the siLUM and anti-LUM groups (Figures 3B, C). Taking a step further, in vivo Matrigel plug assays were performed to evaluate the effect of sLUM on angiogenesis. Matrigel containing bFGF was subcutaneously injected into nude mice. bFGF with or without rmLUM was supplemented to the Matrigel plugs every other day. At day 9, the animals were euthanized, and Matrigel plugs were isolated for capillary density analysis. By immunohistochemical analysis with CD31 staining, increased microvessel density was observed in the rmLUM treatment group (Figure 3D). The effect of anti-LUM on rmLUM-induced angiogenesis was also evaluated. From our experimental findings, microvessel density was decreased upon anti-LUM administration (Figure 3E). Besides, we observed upregulation of VEGFA by rhLUM in HCC cells (Figure 3F), as accompanied by an upregulation of VEGFR1/2 in rhLUM-treated HUVEC (Figure 3G). The changes in expression of angiogenic factors and receptors further supported the role of sLUM on angiogenesis.

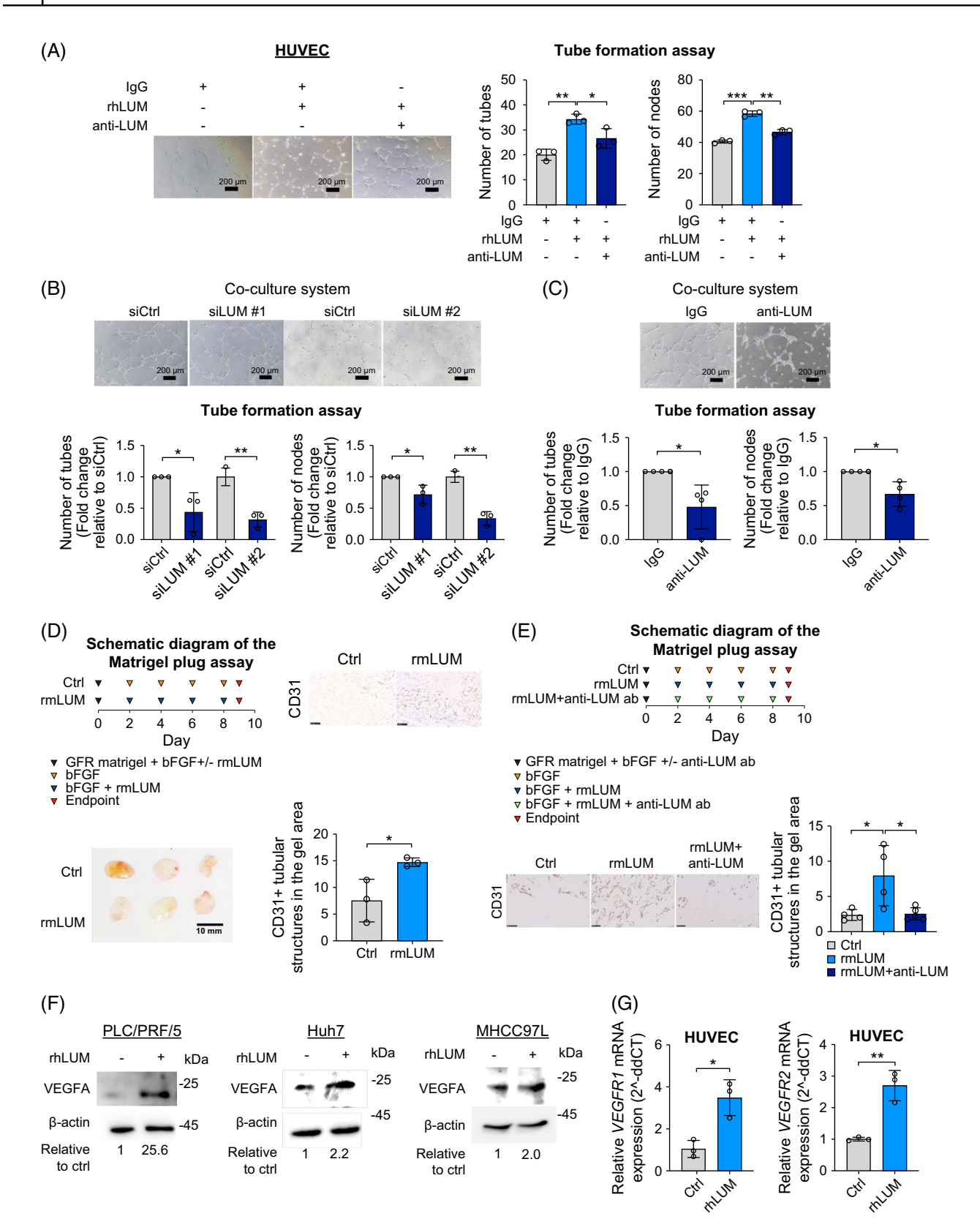


FIGURE 3 Secreted lumican enhances angiogenesis. (A) Effect of rhLUM with or without anti-LUM antibody (2 μg/mL) on angiogenesis as determined by tube formation assay with HUVEC (n = 3). Scale bar: 200 μm. (B) Tube formation assay in HUVEC co-cultured with siCtrl or siLUM liver fibroblasts (n = 3 for siLUM #1). Representative data of siLUM #2 is shown. The experiment was performed twice, each in triplicate. Scale bar: 200 μm. (C) Tube formation assay in HUVEC co-cultured with liver fibroblasts treated with IgG control or anti-LUM antibody (2 μg/mL) (n = 4). Scale bar: 200 μm. (D) Effect of recombinant mouse lumican (rmLUM) on angiogenesis as determined by Matrigel plug in vivo assay. Schematic diagram of the Matrigel plug assay (*upper left*). Image of the Matrigel plugs isolated from the Ctrl and rmLUM treatment group (*lower left*). Scale

Secreted lumican promotes self-renewal and tumor initiation of HCC

Thus far, our experimental findings suggest that sLUM enhances metastatic potential and angiogenesis, 2 major cellular steps implicated in tumor progression. To understand if sLUM exerts any effects on the selfrenewal ability of HCC, the tumorsphere formation assay was performed. From our results, rhLUM enhanced tumorsphere formation of HCC cells, and the effect was abrogated by co-treating HCC cells with anti-LUM (Figure 4A). The findings suggested that sLUM promoted self-renewal in vitro and were substantiated by results with the 2 co-culture setups as described above. Tumorsphere formation was suppressed in HCC cells co-cultured with LF after silencing lumican (versus LF transfected with siCtrl) (Figure 4B), and in HCC cells co-cultured with LF treated with anti-LUM (vs. LF treated with IgG) (Figure 4C). The encouraging findings led us to further explore the effect of sLUM on in vivo tumorigenicity. HCC cell lines (Huh7 and MHCC97L) and PDX1 cells established from a clinical HCC sample were injected subcutaneously into NOD/SCID mice. rhLUM was supplemented subcutaneously to the tumor injection site, and tumor incidence was measured. At the experimental endpoint, a higher tumor incidence and T-IC frequency were consistently observed in the rhLUM treatment group for both HCC cell line-derived xenografts as well as for the patient-derived xenograft (Figure 4D and Table 1).

Secreted lumican triggers the AKT/GSK3β/ β-catenin signaling cascade

To decipher the downstream molecular mechanisms mediating the functions of sLUM in HCC, we carried out transcriptomic profiling and proteomic profiling with tumor lysates collected from the MHCC97L animal model and cell line model, respectively. From the RNA-seq results, based on differential expression analysis between the rhLUM-treated and Ctrl groups, a total of 1502 protein-coding genes were differentially expressed [False discovery rate (FDR) < 0.05, I

Log₂fold change (FC) $l \ge 1$]. The distribution of identified genes was displayed in a volcano plot (Figure 5A). Of these differentially expressed genes (DEGs), a total of 690 genes were upregulated and 812 genes were downregulated in the rhLUM treatment group (Supplemental Table S1, http://links.lww.com/HC9/C59). To investigate the mechanistic connection of the DEGs in tumorigenesis, the upregulated DEGs were subjected to GO enrichment analysis. Results showed that multiple pathways crucial in tumorigenesis were enriched, includina Wnt signaling and MAPK (Figure 5B). By proteomic profiling with LC-MS/MS, a total of 438 proteins (p < 0.05, FC ≥ 1.2 , and FC ≤ 0.83) were differentially expressed in the rhLUM-treated MHCC97L cells. Among the differentially expressed proteins (DEPs), a total of 281 proteins (FC > 1.2) were upregulated (Supplemental Table S2, http://links.lww. com/HC9/C59). Reactome gene set enrichment analyses of the upregulated DEPs were conducted to acquire mechanistic insight into the upregulated DEPs in the pathway related to tumorigenesis (Figure 5C). Notably, enrichment of Wnt signaling was detected in both RNAseq and Reactome gene set analyses. To verify whether Wnt signaling is altered in HCC in response to sLUM, β-catenin expression was first examined in the rhLUM-treated HCC cell lines, as well as the PDX1 tumor lysates harvested from the mouse model (depicted in Figure 4D). Results from western blotting confirmed the increase of β-catenin expression in the nuclear fractions of the HCC cells upon rhLUM treatment (Figure 5D).

To test whether the functional effects of lumican are mediated through β -catenin signaling in HCC cells and HUVEC, we employed β -catenin inhibitor CWP232228 upon rhLUM treatment in the tumorsphere formation assay and tube formation assay. CWP232228 is a selective small molecular inhibitor that targets the binding of β -catenin to the T-cell factor protein in the nucleus, thereby suppressing a subset of β -catenin-responsive gene expression. With the assays, tumorsphere formation and tube formation were attenuated upon co-treatment of CWP232228 (Figure 6A). The reversal effect of CWP232228 on rhLUM-induced pro-tumorigenic functions in HCC cells

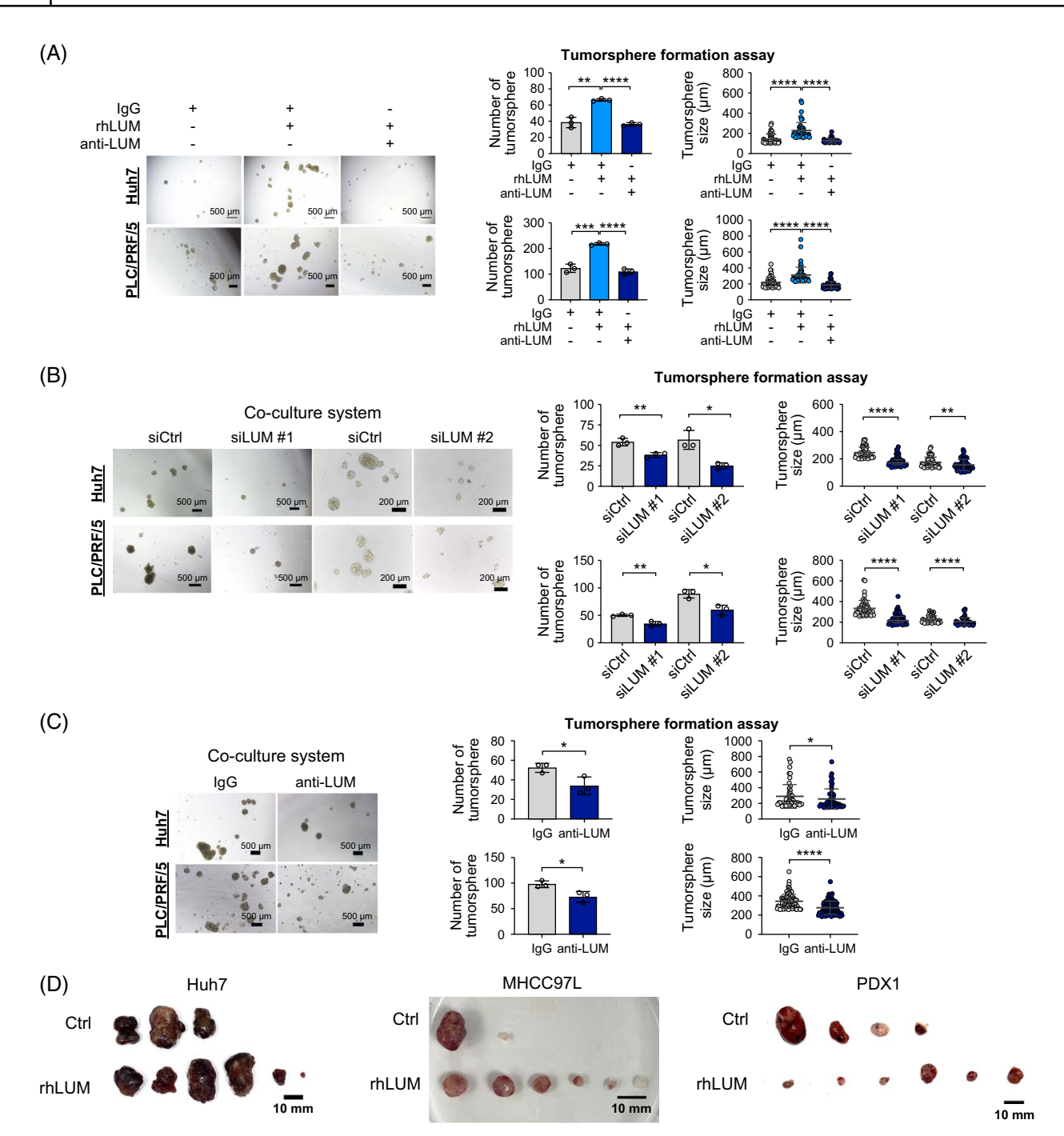


FIGURE 4 Secreted lumican promotes self-renewal and tumor initiation of HCC. (A) Tumorsphere assays in Huh7 (*upper*) and PLC/PRF/5 (*lower*) cells treated with rhLUM (2 μg/mL) or in combination of rhLUM (2 μg/mL) and anti-LUM antibody (2 μg/mL). Representative data is shown. The experiment was performed twice, each in triplicate. Scale bar: 500 μm. (B) Tumorsphere assays in Huh7 (*upper*) and PLC/PRF/5 (*lower*) cells co-cultured with liver fibroblasts (LFs), siCtrl, or siLUM cells. Representative data are shown. The experiment was performed twice, each in triplicate. Scale bar: 500 μm for siLUM #1 or 200 μm for siLUM #2. (C) Tumorpshere assays in Huh7 (*upper*) and PLC/PRF/5 (*lower*) cells co-cultured with LF treated with IgG control or anti-LUM antibody (2 μg/mL). Representative data is shown. The experiment was performed twice, each in triplicate. Number of tumorsphere: unpaired *t* test. Tumorsphere size: Mann–Whitney *U* test. Scale bar: 500 μm. (D) Images of the Huh7 (*left*), MHCC97L (*middle*), and PDX1 (*right*) tumors harvested from the mice treated with or without rhLUM. No HCC tumor was identified in the nodule on the right from the MHCC97L-Ctrl group upon histological examination. Scale bar: 10 mm. Data represents mean ± SD. *p < 0.05, **p < 0.001, ***p < 0.001, and *****p < 0.0001. Abbreviations: anti-LUM, anti-lumican antibody; Ctrl, control; LFs, liver fibroblasts; rhLUM, recombinant human lumican; siCtrl, negative control siRNA; siLUM, lumican siRNA.

TABLE 1 Tumor incidence and estimated T-IC frequency of MHCC97L cell line-derived, Huh7 cell line-derived, and HCC patient-derived xenografts treated with or without recombinant human lumican protein

	Tumor incidence	Estimated T-IC frequency
MHCC97L-Ctrl	1/6	1/5485
MHCC97L-rhLUM	6/6	1/1
Huh7-Ctrl	3/8	1/10638
Huh7-rhLUM	6/8	1/3607
PDX1-Ctrl	4/6	1/9102
PDX1-rhLUM	6/6	1/1

Abbreviations: Ctrl, control; PDX, patient-derived xenograft; rhLUM, recombinant human lumican; T-IC, tumor-initiating cell.

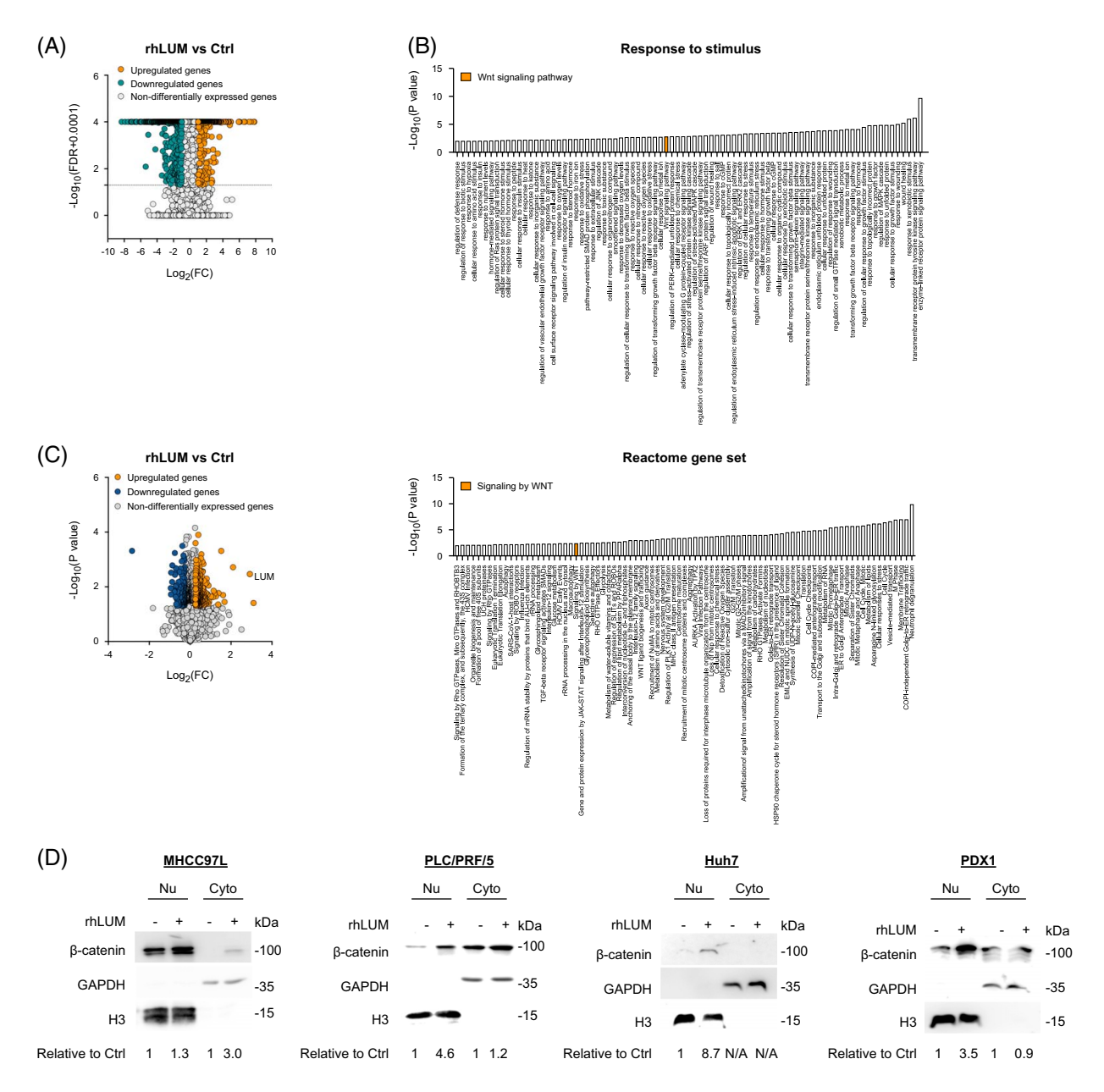
and HUVEC implied the involvement of β-catenin signaling in the actions of sLUM. From the literature review, VEGFA is a downstream effector of β-catenin in HCC.[25,26] Considering the reversal effect of CWP232228 on rhLUM-induced tube formation, expression of VEGFA was examined in HCC cells upon co-administration of CWP232228 to assess whether the effect of rhLUM on VEGFA expression was mediated through β-catenin. By western blotting, expression of VEGFA in HCC cells was diminished upon co-treatment with CWP232228 when compared to HCC cells treated with rhLUM only (Figure 6B). Next, we sought to understand how lumican regulates the Wnt signaling pathway. To address this question, we examined the expressions of major upstream intrinsic players implicated in the pathway activation. Expressions of Wnt3a and pLRP6, key biomarkers reflecting ligand-receptor activity in the Wnt/β-catenin pathway, were unaltered upon rhLUM treatment (Supplemental Figures S4A, B, http://links.lww.com/ HC9/C59), suggesting that the augmented nuclear βcatenin expression could be mediated by other interconnected pathways. From previous studies, crosstalk between PI3K/AKT and β-catenin signaling has been illustrated in HCC.[27-31] Hence, we specuthat nuclear β-catenin expression upregulated via PI3K/AKT pathway in response to lumican in HCC. To this end, the expression of pAKT and pGSK3β was examined upon rhLUM treatment in HCC cells. Interestingly, upregulated pAKT(Ser473) and pGSK3β(Ser9) expressions were observed in rhLUM-treated cells (Figure 6C). To corroborate the link between lumican and PI3K/AKT pathway at a functional level, AKT inhibitor MK2206 (AKTi) was employed in in vitro assays. AKTi reversed the rhLUMinduced effects on cell migration, invasion, tumorsphere formation, and tube formation (Figures 6D-F). Besides, expression of nuclear β-catenin, pAKT (Ser473), pGSK3β (Ser9), and VEGFA was attenuated upon administration of AKTi in rhLUM-treated cells

(Figure 6G and Supplemental Figure S5, http://links. lww.com/HC9/C59). The above experimental findings indicated that secreted lumican mediates its protumorigenic effects through activation of pAKT in HCC cells. Lastly, we attempted to explore how secreted lumican interacts with the PI3K/AKT pathway. To this end, we performed a co-immunoprecipitation (co-IP) experiment with pMET (Tyr1234/ 1235), a receptor tyrosine kinase upstream of PI3K/ AKT, in rhLUM-treated HCC cells. The results demonstrated the interaction between pMET (Tyr1234/ 1235) and rhLUM, suggesting that sLUM activated PI3K/AKT signaling through interaction with MET receptor (Supplemental Figure S6, http://links.lww. com/HC9/C59). These findings altogether suggest that sLUM regulates HCC stemness and angiogenesis via the AKT/GSK3β/β-catenin signaling cascade.

DISCUSSION

In the present study, we characterized the functional roles of the secreted lumican in HCC and demonstrated that sLUM exhibited pro-tumorigenic effects on both HCC cells and HUVEC for the induction of metastatic potential, self-renewal ability, and angiogenesis by in vitro and in vivo experiments. Self-renewal ability and tumor initiation are defining hallmarks of cancer stemness and are properties tightly linked to tumor recurrence. Angiogenesis, cell migration, and invasion are phenotypes associated with extrahepatic tumor dissemination. Besides, mechanistic dissection in our study revealed the role of the AKT/GSK3β/β-catenin signaling cascade as a downstream effector for lumican in HCC, and this was consolidated by experiments using AKT and β-catenin inhibitors. A graphic summary of the study findings is presented in Figure 6H.

Apart from unraveling the functional roles of sLUM in HCC, our findings portrayed liver fibroblasts as a major source of sLUM, which possibly exerts its functions on HCC cells in a paracrine manner. This speculation was supported by results with our co-culture models, that lumican is a critical component in the secretome from liver fibroblasts, promoting various tumorigenic phenotypes, including cancer stemness properties and angiogenesis. As a matter of fact, a wide array of ECM proteins, including different types of collagen, glycoproteins, proteoglycans, and polysaccharides, have been reported to contribute to cancer stemness.[32] Mechanistically, ECM proteins were reported to modulate stemness via physical and biochemical properties, control of growth factor release, or metabolic reprogramming.^[32] In this work, we showed that lumican fosters HCC stemness via potentiation of β-catenin, an important mechanism implicated in the regulation of cancer stemness and angiogenesis, [33] including in HCC, as illustrated in previous studies by our group. [34–36]



Transcriptomic and proteomic profiling reveal the enrichment of Wnt signaling in HCC cells treated with recombinant human lumican. (A) Volcano plot of protein-coding genes identified in the subcutaneous MHCC97L tumor harvested from mice treated with recombinant human lumican protein (rhLUM) by RNA-sequencing. Orange dots: upregulated genes (690 genes); green dots: downregulated genes (812 genes); grey dots: non-differentially expressed genes (15,229 genes). A differentially expressed gene is defined as ILog₂(FC)I≥1 and FDR < 0.05. (B) GO enrichment analysis of terms under response to stimulus enriched in upregulated differentially expressed genes in the rhLUM treatment group using Metascape. (C) Volcano plot of proteins identified in the rhLUM-treated MHCC97L cells by LC-MS/MS (left). Orange dots: upregulated proteins (281 proteins); blue dots: downregulated proteins (157 proteins); grey dots: non-differentially expressed proteins (4318 proteins). Differentially expressed proteins are defined as FC \geq 1.2 or FC \leq 0.83 and p < 0.05. Reactome pathways enriched in upregulated differentially expressed proteins in the rhLUM treatment group using Metascape (right). (D) Western blot analysis of β-catenin expression in nuclear (Nu) and cytoplasmic (Cyto) fractions of MHCC97L, PLC/PRF/5, and Huh7 cells treated with or without rhLUM (2 µg/mL, 48 h), as well as PDX1 tumor tissue harvested from a mouse model treated with or without rhLUM. Pooled samples of all PDX1 tumor lysates from each group were used for western blot. Ctrl: untreated cells. Quantification of fold change of β-catenin band intensity in the rhLUM-treated group against the untreated group was indicated beneath the western blot images. H3 and GAPDH were used as the loading control for the nuclear fraction and cytoplasmic fraction, respectively. Representative data of MHCC97L, PLC/PRF/5, and Huh7 cells are shown. The experiment was performed twice. Abbreviations: Ctrl, control; FC, fold change; FDR, false discovery rate; LC-MS/MS, liquid chromatography-tandem mass spectrometry; rhLUM, recombinant human lumican.

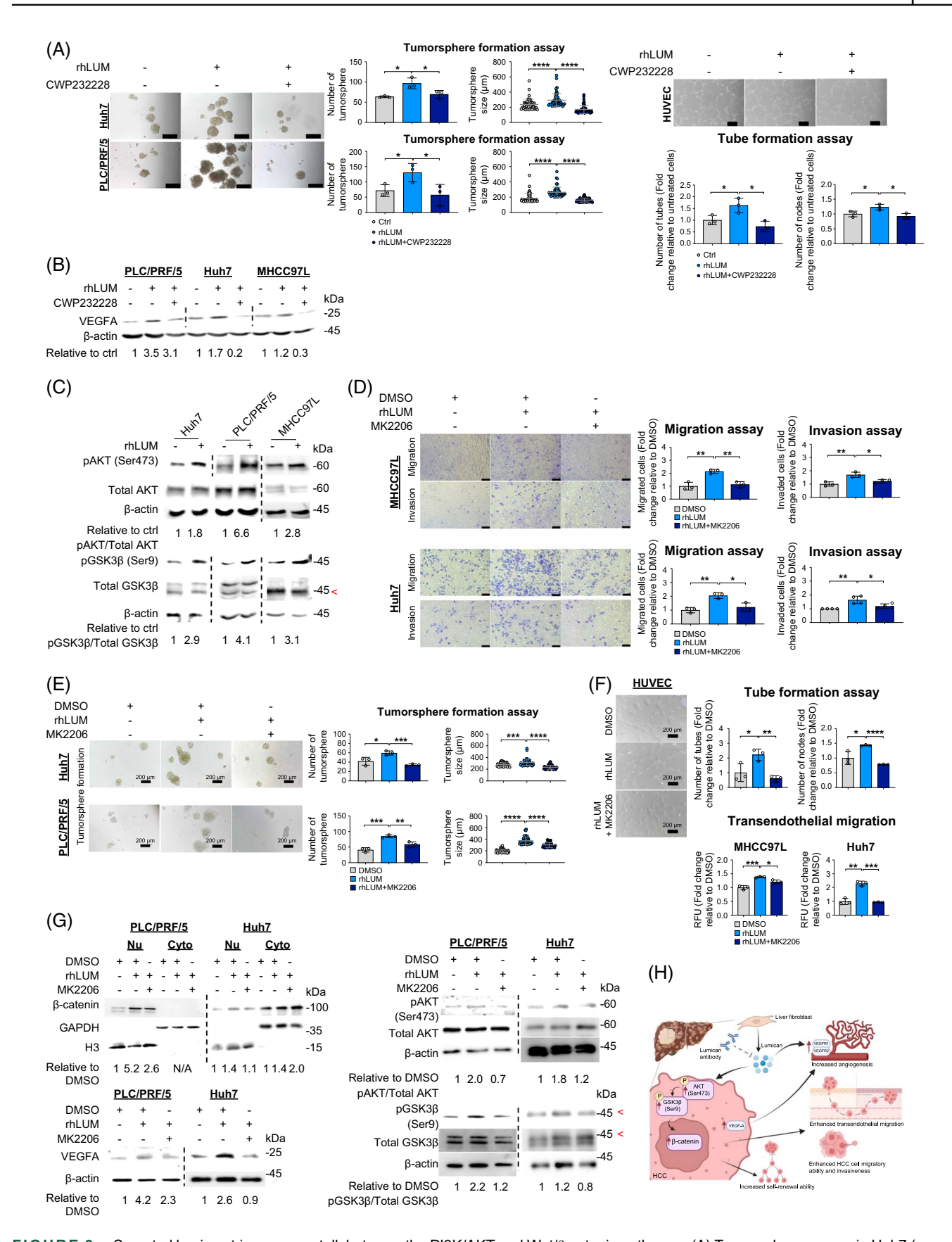


FIGURE 6 Secreted lumican triggers crosstalk between the PI3K/AKT and Wnt/β-catenin pathways. (A) Tumorsphere assays in Huh7 (*upper*) and PLC/PRF/5 (*lower*) cells treated with or without rhLUM (2 µg/mL) or in combination of rhLUM (2 µg/mL) and CWP232228 (0.5 µM). Representative data is shown. The experiment was performed twice, each in triplicate. Scale bar: 300 µm. Tube formation assay in HUVEC (*right*) treated with or without rhLUM (2 µg/mL) or in combination of rhLUM (2 µg/mL) and CWP232228 (2 µM). Scale bar: 200 µm. Representative data

are shown. The experiment was performed twice, each in triplicate. Unpaired t test. Data represents mean ± SD. (B) Western blot analysis of VEGFA expression in PLC/PRF/5, Huh7, and MHCC97L cells treated with rhLUM (2 µg/mL, 48 h) or co-treatment of rhLUM (2 µg/mL, 48 h) and CWP232228 (2 µM, 48 h). Quantification of fold change of VEGFA band intensity in the rhLUM-treated group against the untreated group was indicated beneath the western blot images. β-actin was used as the loading control. Results of the blot with different exposure times were separated by a dashed line. Representative data is shown. The experiment was performed twice. (C) Western blot analysis of pAKT and pGSK3β protein expression in Huh7, PLC/PRF/5, and MHCC97L cells treated with rhLUM (2 µg/mL, 16 h). Quantification of fold change of pAKT and pGSK3 band intensity in the rhLUM-treated group against the untreated group was indicated beneath the western blot images. β-actin was used as the loading control. Results of the blot with different exposure times were separated by a dashed line. The arrow indicated the expected size of the GSK3β. Representative data are shown. The experiment was performed twice. (D) Transwell migration and matrigel invasion assays in MHCC97L (upper) and Huh7 (lower) cells upon rhLUM (2 µg/mL) or in combination of rhLUM (2 µg/mL) and MK2206 (5 µM) treatment. Representative data are shown. The experiment was performed at least twice, each in triplicate. (E) Tumorsphere assays in Huh7 and PLC/PRF/5 cells treated with rhLUM (2 μg/mL) or in combination of rhLUM (2 μg/mL) and MK2206 (5 μM for Huh7; 2 μM for PLC/PRF/5). Representative data is shown. The experiment was performed twice, each in triplicate. Number of tumorsphere: Unpaired t test. Tumorsphere size: Mann-Whitney U test. Scale bar: 200 µm. (F) Effect of rhLUM with or without MK2206 (10 µM) on angiogenesis as determined by tube formation assay with HUVEC (upper). Representative data is shown. Scale bar: 200 µm. The experiment was performed twice, each in triplicate. Transendothelial migration of MHCC97L and Huh7 cells treated with rhLUM (2 μg/mL) or in combination of rhLUM and MK2206 (5 μM) (lower). Representative data are shown. The experiment was performed twice, each in triplicate. Unpaired t test. Data represents mean \pm SD. (G) Western blot analysis of β -catenin expression in nuclear (Nu) and cytoplasmic (Cyto) fractions of PLC/PRF/5 and Huh7 cells treated with DMSO, rhLUM (2 µg/mL, 48 h), or cotreatment of rhLUM (2 µg/mL, 48 h) and MK2206 (5 µM for Huh7; 2 µM for PLC/PRF/5, 48 h) (upper left). H3 and GAPDH were used as the loading control for the nuclear fraction and cytoplasmic fraction, respectively. Western blot analysis of VEGFA expression in PLC/PRF/5 and Huh7 cells treated with rhLUM (2 µg/mL, 48 h) or co-treatment of rhLUM (2 µg/mL, 48 h) and MK2206 (5 µM for Huh7; 2 µM for PLC/PRF/5, 48 h) (lower left). Western blot analysis of pAKT and pGSK3β protein expression in PLC/PRF/5 and Huh7 cells treated with rhLUM (2 μg/mL, 16 h) or co-treatment of rhLUM (2 μg/mL, 16 h) and MK2206 (5 μM for Huh7; 2 μM for PLC/PRF/5, 16 h) (right). β-actin was used as the loading control. The arrow indicated the expected size of the GSK3β. Quantification of fold change of β-catenin, VEGFA, pAKT, and pGSK3β band intensity in the rhLUMtreated group or co-treatment group against the DMSO group was indicated beneath the western blot images. Representative data are shown. Each blot was separated by a dashed line. The experiment was performed twice. (H) Graphical summary of the study. The image is created with BioRender.com. *p < 0.05, **p < 0.01, ***p < 0.001, and ****p < 0.0001. Abbreviation: rhLUM, recombinant human lumican.

Lumican is well-recognized for interacting with integrin at the cell-matrix interface to modulate cell motility.[11,37] Besides, ERK1/2, TGFβ2, FAK, FOXO, and p53 were identified as the downstream mediators for lumican functions in cancer models.^[12,18,20,38-40] In our current study, with RNA-seg and mass spectrometry experiments, the Wnt signaling pathway was consistently identified in both profiling analyses. As a matter of fact, proteoglycans, including biglycan and GPC3, have been reported to modulate the Wnt/β-catenin signaling cascade.[41,42] In particular, GPC3 was reported to bind to frizzled receptors, followed by endocytosis of the GPC3–FZD8 complex upon the induction of Wnt3a.[43] Findings from our current study further substantiate the potential significance of proteoglycans in the regulation of Wnt/β-catenin pathway in human cancers. While CTNNB1 mutation is a major molecular event leading to activation of Wnt/β-catenin pathway, other mechanisms have been reported to trigger the signaling cascade, including overexpression of intrinsic players in the pathway, such as LRP6 and Frizzled 7, as previously reported by our group. [34,36,44] Apart from that, aberrant β-catenin expression could also result from activation of the AKT/GSK3B pathway, in which phosphorylated AKT (at Ser473) leads to the phosphorylation of GSK3β at Ser9, thereby inhibiting the proteasomal degradation of β -catenin. Stabilization of β -catenin is followed by translocation into the nucleus and transcriptional activation of downstream effectors. The crosstalk between PI3K/ AKT and β-catenin signaling pathways was shown to participate in HCC tumor growth, metastasis, and stemness.^[27–31] Besides, AKT/GSK3β/β-catenin signaling

plays a role in tumor angiogenesis.^[30,45] In a very recent report, lumican was shown to take part in AKT/GSK3β/β-catenin signaling in cardiac fibrosis.^[46] Our current study, instead, revealed the role of this signaling cascade in mediating the functions of sLUM in human cancers. In addition, we demonstrated that secreted lumican interacts with MET receptor in HCC cells, a potential mechanism through which lumican activates the PI3K/AKT pathway. Apart from this, from our in vitro experiments, His-tagged rhLUM could be detected in HCC cells using His antibody by western blotting (data not shown), suggesting that internalization of exogenous lumican by HCC is also possible.

The findings in our present study provide some insights from a conceptual point of view. Expression of lumican has been reported in cancer-associated fibroblasts in breast, pancreas, and cervical cancers.[47-49] From our expression analyses of clinical samples, liver fibroblasts from both non-tumor and HCC tumor tissues are a notable source of lumican. Considering the biological nature of lumican as an ECM protein, in this work, we focused on the secreted form of lumican and illustrated its role in self-renewal, tumor initiation, and angiogenesis, apart from metastatic potential in liver cancer. Of relevance to the tumor biology in HCC, early recurrence (within 2 y from curative resection) is believed to result from occult intrahepatic spread of the primary tumor, while late recurrence represents metachronous tumor arising from background chronic liver diseases.^[50] Therefore, our findings may imply that lumican secreted from the fibrotic milieu could possibly promote the self-renewal

ability of microscopic residual HCC cells in the liver after tumor resection, increasing the chance of tumor recurrence. Our findings also carry potential implications of clinical relevance. First, lumican could be a prognostic biomarker of HCC. As mentioned in the Introduction section, the degree of fibrosis from the non-tumor liver tissue is a prognosticator of HCC. In this connection, evaluation of lumican level in the nontumor liver tissue in HCC patients could provide further information to stratify patients' prognosis. Secondly, in this study, we illustrated that the actions of lumican are potentially targetable by the antibody approach. Therefore, lumican could be an actionable target for preventing tumor recurrence and extrahepatic metastasis by means of antibody or emerging approaches such as aptamers as (neo)adjuvant therapy. In this regard, lumican expression level in liver tissues from HCC patients is a potential biomarker to inform therapeutic decisions. With the known undesirable off-pathway effects and toxicity of AKT and β-catenin inhibitors, targeting alternative novel regulators of the signaling cascade in a disease-specific context is a promising direction for research and development. The therapeutic values of anti-LUM therapy in HCC await further in-depth evaluation.

DATA AVAILABILITY STATEMENT

The data from the TCGA-LIHC cohort analyzed in this study were obtained from UCSC Xena at https://xena.ucsc.edu/. The results published here are in part based upon data generated by the TCGA Research Network: https://www.cancer.gov/tcga. The data from single-cell RNA-seq analyzed in this study were obtained from GepLiver at http://www.gepliver.org/#/explore/. The RNA-seq data generated in this study are available in Gene Expression Omnibus (GEO) at GSE268858 (https://www.ncbi.nlm.nih.gov/geo/query/acc.cgi?acc = GSE268858). The datasets used and/or analyzed during the current study are available from the corresponding author on reasonable request.

AUTHOR CONTRIBUTIONS

Conception and design: Regina Cheuk-Lam Lo. Data acquisition: Kristy Kwan-Shuen Chan, Cheuk-Yan Wong, Kwan-Yung Au, Long-Hin Suen, Wai-Wai Yip, Jing-Mian Zhang, Eva Yi-Man Fung, Terence Kin-Wah Lee, Irene Oi-Lin Ng, and Tan-To Cheung. Data analysis and interpretation: Kristy Kwan-Shuen Chan, Cheuk-Yan Wong, Kwan-Yung Au, Eva Yi-Man Fung, and Regina Cheuk-Lam Lo. Writing of manuscript: Kristy Kwan-Shuen Chan and Regina Cheuk-Lam Lo. Study supervision: Regina Cheuk-Lam Lo.

FUNDING INFORMATION

This work was supported by the Health and Medical Research Fund, Health Bureau, Hong Kong (08192876),

Seed Fund for Basic Research, HKU (202011159015), and Research Assessment Exercise 2026 Development Fund, HKU.

ACKNOWLEDGMENTS

Assistance with the study: The authors thank the Centre of Comparative Medical Research and Centre for PanorOmic Sciences, LKS Faculty of Medicine, HKU, for technical support.

Presentation: none.

CONFLICTS OF INTEREST

The authors have no conflicts to report.

ORCID

Regina Cheuk-Lam Lo https://orcid.org/0000-0001-6213-0343

REFERENCES

- Wang Q, Fiel MI, Blank S, Luan W, Kadri H, Kim KW, et al. Impact of liver fibrosis on prognosis following liver resection for hepatitis B-associated hepatocellular carcinoma. Br J Cancer. 2013;109:573–81.
- Zhang Y, Wang R, Yang X. FIB-4 index serves as a noninvasive prognostic biomarker in patients with hepatocellular carcinoma: A meta-analysis. Medicine (Baltimore). 2018;97:e13696.
- Qi M, Chen Y, Zhang GQ, Meng YJ, Zhao FL, Wang J, et al. Clinical significance of preoperative liver stiffness measurements in primary HBV-positive hepatocellular carcinoma. Future Oncol. 2017;13:2799–810.
- Baghy K, Tatrai P, Regos E. Proteoglycans in liver cancer. World J Gastroenterol. 2016;22:379–93.
- Krishnan A, Li X, Kao WY, Viker K, Butters K, Masuoka H, et al. Lumican, an extracellular matrix proteoglycan, is a novel requisite for hepatic fibrosis. Lab Invest. 2012;92:1712–25.
- Furuta K, Sato S, Yamauchi T, Ozawa T, Harada M, Kakumu S. Intrahepatic gene expression profiles in chronic hepatitis B and autoimmune liver disease. J Gastroenterol. 2008;43: 866–74.
- Charlton M, Viker K, Krishnan A, Sanderson S, Veldt B, Kaalsbeek AJ, et al. Differential expression of lumican and fatty acid binding protein-1: New insights into the histologic spectrum of nonalcoholic fatty liver disease. Hepatology. 2009;49: 1375–84.
- Decaris ML, Li KW, Emson CL, Gatmaitan M, Liu S, Wang Y, et al. Identifying nonalcoholic fatty liver disease patients with active fibrosis by measuring extracellular matrix remodeling rates in tissue and blood. Hepatology. 2017;65:78–88.
- Berdiaki A, Giatagana EM, Tzanakakis G, Nikitovic D. The landscape of small leucine-rich proteoglycan impact on cancer pathogenesis with a focus on biglycan and lumican. Cancers (Basel). 2023;15:3549.
- Giatagana EM, Berdiaki A, Tsatsakis A, Tzanakakis GN, Nikitovic D. Lumican in carcinogenesis-revisited. Biomolecules. 2021;11:1318.
- Nikitovic D, Papoutsidakis A, Karamanos NK, Tzanakakis GN. Lumican affects tumor cell functions, tumor-ECM interactions, angiogenesis and inflammatory response. Matrix Biol. 2014;35: 206–14.
- Salcher S, Spoden G, Huber JM, Golderer G, Lindner H, Ausserlechner MJ, et al. Repaglinide silences the FOXO3/ lumican axis and represses the associated metastatic potential of neuronal cancer cells. Cells. 2020;9:1.

- Hsiao KC, Chu PY, Chang GC, Liu KJ. Elevated expression of lumican in lung cancer cells promotes bone metastasis through an autocrine regulatory mechanism. Cancers (Basel). 2020;12: 233.
- Mao W, Luo M, Huang X, Wang Q, Fan J, Gao L, et al. Knockdown of lumican inhibits proliferation and migration of bladder cancer. Transl Oncol. 2019;12:1072–8.
- Karamanou K, Franchi M, Onisto M, Passi A, Vynios DH, Brézillon S. Evaluation of lumican effects on morphology of invading breast cancer cells, expression of integrins and downstream signaling. FEBS J. 2020;287:4862–80.
- Karamanou K, Franchi M, Vynios D, Brézillon S. Epithelial-tomesenchymal transition and invadopodia markers in breast cancer: Lumican a key regulator. Semin Cancer Biol. 2020;62: 125–33.
- Yamamoto T, Matsuda Y, Kawahara K, Ishiwata T, Naito Z. Secreted 70kDa lumican stimulates growth and inhibits invasion of human pancreatic cancer. Cancer Lett. 2012;320:31–9.
- Tan Y, Zhou Y, Zhang W, Wu Z, Xu Q, Wu Q, et al. Repaglinide restrains HCC development and progression by targeting FOXO3/lumican/p53 axis. Cell Oncol (Dordr). 2024;47: 1167–81.
- Li X, Truty MA, Kang Y, Chopin-Laly X, Zhang R, Roife D, et al. Extracellular lumican inhibits pancreatic cancer cell growth and is associated with prolonged survival after surgery. Clin Cancer Res. 2014;20:6529–40.
- Wang X, Zhou Q, Yu Z, Wu X, Chen X, Li J, et al. Cancerassociated fibroblast-derived Lumican promotes gastric cancer progression via the integrin beta1–FAK signaling pathway. Int J Cancer. 2017;141:998–1010.
- Lo J, Lau EYT, Ching RHH, Cheng BYL, Ma MKF, Ng IOL, et al. Nuclear factor kappa B-mediated CD47 up-regulation promotes sorafenib resistance and its blockade synergizes the effect of sorafenib in hepatocellular carcinoma in mice. Hepatology. 2015; 62:534–45
- Ma MKF, Lau EYT, Leung DHW, Lo J, Ho NPY, Cheng LKW, et al. Stearoyl-CoA desaturase regulates sorafenib resistance via modulation of ER stress-induced differentiation. J Hepatol. 2017;67: 979–90.
- Hu Y, Smyth GK. ELDA: Extreme limiting dilution analysis for comparing depleted and enriched populations in stem cell and other assays. J Immunol Methods. 2009;347:70–8.
- Jang GB, Hong IS, Kim RJ, Lee SY, Park SJ, Lee ES, et al. Wnt/ beta-catenin small-molecule inhibitor CWP232228 preferentially inhibits the growth of breast cancer stem-like cells. Cancer Res. 2015;75:1691–702.
- Xie P, Yu M, Zhang B, Yu Q, Zhao Y, Wu M, et al. CRKL dictates anti-PD-1 resistance by mediating tumor-associated neutrophil infiltration in hepatocellular carcinoma. J Hepatol. 2024;81: 93–107.
- Qu B, Liu BR, Du YJ, CHEN J, CHENG YQ, XU W, et al. Wnt/ beta-catenin signaling pathway may regulate the expression of angiogenic growth factors in hepatocellular carcinoma. Oncol Lett. 2014;7:1175–8.
- Zhuang L, Wang X, Wang Z, Ma X, Han B, Zou H, et al. MicroRNA-23b functions as an oncogene and activates AKT/ GSK3beta/beta-catenin signaling by targeting ST7L in hepatocellular carcinoma. Cell Death Dis. 2017;8:e2804.
- Zhang CZ, Chen SL, Wang CH, He YF, Yang X, Xie D, et al. CBX8 exhibits oncogenic activity via AKT/beta-catenin activation in hepatocellular carcinoma. Cancer Res. 2018;78:51–63.
- Wang C, Cao F, Cao J, Jiao Z, You Y, Xiong Y, et al. CD58 acts as a tumor promotor in hepatocellular carcinoma via activating the AKT/GSK-3beta/beta-catenin pathway. J Transl Med. 2023; 21:539.
- Song M, Pan Q, Yang J, He J, Zeng J, Cheng S, et al. Galectin-3 favours tumour metastasis via the activation of beta-catenin

- signalling in hepatocellular carcinoma. Br J Cancer. 2020;123: 1521–34
- Yu H, Zhou L, Loong JHC, Lam KH, Wong TL, Ng KY, et al. SERPINA12 promotes the tumorigenic capacity of HCC stem cells through hyperactivation of AKT/beta-catenin signaling. Hepatology. 2023;78:1711–26.
- Nallanthighal S, Heiserman JP, Cheon DJ. The role of the extracellular matrix in cancer stemness. Front Cell Dev Biol. 2019;7:86.
- Olsen JJ, Pohl SÖ, Deshmukh A, Visweswaran M, Ward NC, Arfuso F, et al. The role of Wnt signalling in angiogenesis. Clin Biochem Rev. 2017;38:131–42.
- Leung CON, Mak WN, Kai AKL, Chan KS, Lee TKW, Ng IOL, et al. Sox9 confers stemness properties in hepatocellular carcinoma through Frizzled-7 mediated Wnt/beta-catenin signaling. Oncotarget. 2016;7:29371–86.
- Leung RWH, Lee TKW. Wnt/beta-catenin signaling as a driver of stemness and metabolic reprogramming in hepatocellular carcinoma. Cancers (Basel). 2022;14:5468.
- Lo RCL, Leung CON, Chan KKS, Ho DWH, Wong CM, Lee TKW, et al. Cripto-1 contributes to stemness in hepatocellular carcinoma by stabilizing Dishevelled-3 and activating Wnt/betacatenin pathway. Cell Death Differ. 2018;25:1426–41.
- Brézillon S, Pietraszek K, Maquart FX, Wegrowski Y. Lumican effects in the control of tumour progression and their links with metalloproteinases and integrins. FEBS J. 2013;280:2369–81.
- Nikitovic D, Berdiaki A, Zafiropoulos A, Katonis P, Tsatsakis A, Karamanos NK, et al. Lumican expression is positively correlated with the differentiation and negatively with the growth of human osteosarcoma cells. FEBS J. 2008;275:350–61.
- Nikitovic D, Chalkiadaki G, Berdiaki A, Aggelidakis J, Katonis P, Karamanos NK, et al. Lumican regulates osteosarcoma cell adhesion by modulating TGFbeta2 activity. Int J Biochem Cell Biol. 2011;43:928–35.
- Papoutsidakis A, Giatagana E, Berdiaki A, Spyridaki I, Spandidos D, Tsatsakis A, et al. Lumican mediates HTB94 chondrosarcoma cell growth via an IGF-IR/Erk1/2 axis. Int J Oncol. 2020; 57:791–803.
- 41. Li N, Wei L, Liu X, Bai H, Ye Y, Li D, et al. A frizzled-like cysteinerich domain in glypican-3 mediates Wnt binding and regulates hepatocellular carcinoma tumor growth in mice. Hepatology. 2019;70:1231–45.
- Berendsen AD, Fisher LW, Kilts TM, Owens RT, Robey PG, Gutkind JS, et al. Modulation of canonical Wnt signaling by the extracellular matrix component biglycan. Proc Natl Acad Sci U S A. 2011;108:17022–7.
- Capurro M, Martin T, Shi W, Filmus J. Glypican-3 binds to Frizzled and plays a direct role in the stimulation of canonical Wnt signaling. J Cell Sci. 2014;127:1565–75.
- Tung EKK, Wong BYC, Yau TO, Ng IOL. Upregulation of the Wnt co-receptor LRP6 promotes hepatocarcinogenesis and enhances cell invasion. PLoS One. 2012;7:e36565.
- He F, Chen H, Yang P, Wu Q, Zhang T, Wang C, et al. Gankyrin sustains PI3K/GSK-3beta/beta-catenin signal activation and promotes colorectal cancer aggressiveness and progression. Oncotarget. 2016;7:81156–71.
- Zhang X, Cui S, Ding Y, Li Y, Wu B, Gao J, et al. Downregulation of B4GALT5 attenuates cardiac fibrosis through Lumican and Akt/GSK-3beta/beta-catenin pathway. Eur J Pharmacol. 2024; 963:176263.
- Leygue E, Snell L, Dotzlaw H, Hole K, Hiller-Hitchcock T, Roughley PJ, et al. Expression of lumican in human breast carcinoma. Cancer Res. 1998;58:1348–52.
- Ping Lu Y, Ishiwata T, Asano G. Lumican expression in alpha cells of islets in pancreas and pancreatic cancer cells. J Pathol. 2002;196:324–30.

- Naito Z, Ishiwata T, Kurban G, Teduka K, Kawamoto Y, Kawahara K, et al. Expression and accumulation of lumican protein in uterine cervical cancer cells at the periphery of cancer nests. Int J Oncol. 2002;20:943–8.
- Imamura H, Matsuyama Y, Tanaka E, Ohkubo T, Hasegawa K, Miyagawa S, et al. Risk factors contributing to early and late phase intrahepatic recurrence of hepatocellular carcinoma after hepatectomy. J Hepatol. 2003;38:200–7.

How to cite this article: Chan KK, Wong C, Au K, Suen L, Yip W, Zhang J, et al. Secreted lumican from the tumor microenvironment potentiates HCC stemness and progression. Hepatol Commun. 2025;9:e0778. https://doi.org/10.1097/HC9.0000000000000000778